ChemPubSoc Europe
DOI: 10.1002/open.201900136
Open Access ChemistryOPEN Communications

Resolution Enhancement in SEA XLOC for Heteronuclear NMR Long-Range Correlation

Tamás Gyöngyösi,[a] Katalin E. Kövér,*[a] and Ole W. Sørensen*[b]

It is shown how the resolution in SEA XLOC NMR spectra for distinguishing between heteronuclear two- and three-bond correlations for all ^{13}C multiplicities can be improved by a modified experiment delivering absorptive profiles in the indirect dimension. The method is demonstrated with applications to ibuprofen and strychnine.

In a recent report,[1] a two-dimensional method, SEA XLOC, was introduced for distinguishing between two- and three-bond heteronuclear long-range correlations in NMR spectroscopy. The distinction is based on different multiplet widths of zero-quantum (ZQ or echo) and double-quantum (2Q or antiecho) signals in the indirect dimension of a 2D spectrum of e.g. a $^{1}H–^{13}C$ correlation one. For three-bond correlations associated with a negative passive $^{2}J_{CH}$ coupling constant, the ZQ multiplet width is larger than the corresponding 2Q multiplet width, because $^{3}J_{HH}-^{2}J_{CH}$ enters into the former whereas $^{3}J_{HH}+^{2}J_{CH}$ enters into the latter. For two-bond correlations associated with positive passive $^{3}J_{CH}$ coupling constant it is opposite, with $^{3}J_{HH}-^{3}J_{CH}$ and $^{3}J_{HH}+^{3}J_{CH}$ entering into the ZQ and 2Q multiplet widths, respectively.

A potential drawback of SEA XLOC is that, in order to access these multiplet widths, ZQ and 2Q or echo and antiecho spectra must be kept and inspected separately. Thus the common feature of most multidimensional experiments of combining echo and antiecho data to obtain pure absorption peakshapes is not an option in SEA XLOC in which the spectra as a consequence are displayed in absolute-value mode to date. Absolute-value peakshapes include dispersive contributions and are therefore wider than pure absorption peakshapes.

The need to keep echo and antiecho or negative and positive ^{13}C frequency contributions separate in order to reveal the two-/three-bond distinction makes it appear impossible to obtain absorptive peak profiles in SEA XLOC. However, there is a way around this apparent dilemma because there is another pool of echo and antiecho data not used in the first absolute-value implementation of SEA XLOC.

In operator terms, the SEA XLOC antiecho and echo parts are in the evolution period represented by I^-S^- and I^-S^+, respectively, with I referring to ^{1}H and S to ^{13}C. In the experiment, the chemical shift contribution from the I^- operators is suppressed in the t_1 period in order to have pure ^{13}C frequencies arising from the $S^-$and S^+ operators and with multiple-quantum multiplet structures in F_1 of the 2D spectrum. The other pool of these S operators are contained in the mirror partners of I^-S^- and I^-S^+, namely I^+S^+ and I^+S^-, and they can be picked up in another experiment. I^-S^- and I^+S^+ have the same multiplet structure and likewise for I^-S^+ and I^+S^-, because the former are both double-quantum coherences and the latter are both zero-quantum coherences. Thus echo/antiecho pairs necessary for absorptive profiles can be formed by combining I^-S^- data with I^+S^+ data and I^-S^+ with I^+S^-. Figure 1 shows how the data associated with the different two-spin coherences are combined to obtain absorptive profiles. Also shown are the associated coherence transfer pathways including the final point to take into account, namely that quadrature detection only detects I^- operators in t_2, so the I^+ operators must be converted to I^- by a π^I pulse at the interface between the evolution and detection periods of the 2D experiment.

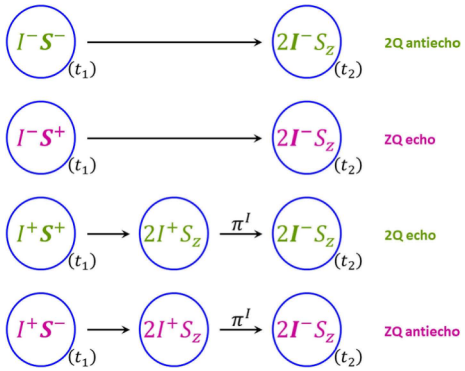

Figure 1. Illustration of coherence transfer pathways and associated operators for obtaining absorptive profiles along the F_1 dimension of the SEA XLOC 2D spectrum, as described in the text. The first two lines refer to the pulse sequence without the dashed π^H pulse in Figure 2 whilst the remaining two lines refer to the version with that pulse included. Echo data from the first experiment are combined with antiecho data from the second and vice versa. Active operators are in boldface.

[a] *T. Gyöngyösi, Prof. Dr. K. E. Kövér*
Department of Inorganic and Analytical Chemistry
University of Debrecen
Egyetem tér 1, H-4032 Debrecen, Hungary
E-mail: kover@science.unideb.hu
[b] *Dr. O. W. Sørensen*
Copenhagen, Denmark
E-mail: sorensen.ole.w@gmail.com

Supporting information for this article is available on the WWW under https://doi.org/10.1002/open.201900136

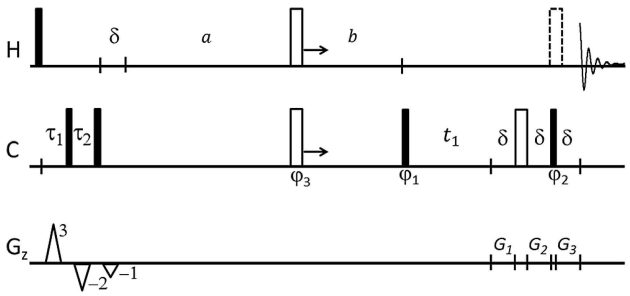

Figure 2. Pulse sequences for F_1 *absorptive* SEA XLOC employing a 2nd order low-pass *J* filter. The version without the final dashed π^H pulse selects two-spin coherences containing H^- and the version with the final dashed π^H pulse included selects two-spin coherences containing H^+ during t_1. Filled and open bars refer to $\pi/2$ and π pulses, respectively. $\tau_1 = 0.5[^1J_{min} + 0.146\,(^1J_{max} - {}^1J_{min})]^{-1}$, $\tau_2 = 0.5[^1J_{max} - 0.146\,(^1J_{max} - {}^1J_{min})]^{-1}$. $\varphi_1 = \{x, -x, -x, x\}$, $\varphi_2 = \{x, x, -x, -x\}$, $\varphi_3 = x$ and alternating receiver phase $\{x, -x\}$. The phase cycle can be repeated with $\varphi_3 = -x$. Δ is the delay for evolution under heteronuclear long-range couplings, δ a gradient delay, and $t_1^{max} < \Delta + \tau_1 + \tau_2 - 2\delta - t(180(C))$. The delays *a* and *b* are $(\Delta + t(180(C)) - \tau_1 - \tau_2 + t_1)/2$ and $(\Delta - t(180(C)) + \tau_1 + \tau_2 - t_1)/2 - \delta$, respectively. Selection of the coherences $\{H^-C^-\}$, $\{H^+C^+\}$, $\{H^-C^+\}$, $\{H^+C^-\}$ in t_1 is done by the gradient triples $\{G_1,G_2,G_3\} = \{-3; 5/2; 15/8\}$, $\{3; -5/2; 15/8\}$, $\{5/2; -3; 15/8\}$, $\{-5/2; 3; 15/8\}$, respectively. The amplitude of the first three gradients is set an order of magnitude lower than the amplitude of the other ones selecting coherence transfer echo or antiecho. It is an option to place a $(\pi/2)_{-x}(\pi/2)_x$ pulse pair at the point of the dashed π^H pulse in the version without that pulse in order to apply equal rf power in both experiments.

The SEA XLOC pulse sequence based on the I^-S^- and I^-S^+ operators is outlined in Figure 2 and does not include the final dashed π^H pulse, in contrast to the one based on the I^+S^- and I^+S^+ operators including that pulse.

The experiment in Figure 2, however, cannot deliver full 2D pure absorption peakshapes and the reason is the same as the equivalent one for the HMBC experiment which is somewhat related to SEA XLOC. The J_{HH} coupling constants cause evolution during the entire time between the first $\pi/2$ pulse and the start of the t_2 period resulting in mixed phases across multiplets in F_2. The procedure developed for HMBC of combining echo and antiecho data and discarding the dispersive part after the Fourier transformation along t_1 prior to Fourier transformation along t_2 and absolute-value calculation[2] is equally applicable to the new SEA XLOC experiment in Figure 2. The result is absorptive profiles in the indirect dimension of the 2D spectrum.

In order to compare the experiment in Figure 2 with the earlier SEA XLOC pulse sequence[1] it must be kept in mind that the former for a given phase cycle requires twice as many scans per t_1 increment as the latter. Thus for the same instrument time the choice is between running the experiment in Figure 2 with a given set of parameters or the earlier version with the same parameters and twice the number of t_1 increments.

If the width at half height of an absorptive Lorentzian line is λ the corresponding width for the line in absolute-value mode is $\sqrt{3} \cdot \lambda$. Therefore, it is relevant to distinguish the two regimes of coarse and high resolution. High resolution shall refer to the case in which a multiplet in a spectrum is displayed with approximately its natural width. On the other hand, coarse resolution shall refer to the case where a multiplet in a spectrum appears broader than its natural width due to only a small number of recorded t_1 increments.

In the limit of high resolution, there is no benefit from doubling the number of t_1 increments in the earlier implementation of SEA XLOC[1] compared to the version in Figure 2 that therefore is expected to offer the best spectral resolution in that regime. In the limit of coarse resolution with double number of t_1 increments in the earlier implementation of SEA XLOC[1] the line widths of λ and $\sqrt{3} \cdot \lambda$ above in principle become λ and $\sqrt{0.75} \cdot \lambda$ indicating similar resolution in the two alternative implementations.

Figures 3 and 4 show excerpts of SEA XLOC spectra of ibuprofen (left in Scheme 1) obtained with the earlier SEA XLOC pulse sequence[1] (referred to as *F_1-magnitude*) and with the new experiment in Figure 2 (referred to as *F_1-absorptive*).

The results are in accordance with the general remarks above. As described in the original paper,[1] the ZQ profile (red) being narrower than the 2Q profile (black) is indicative of a

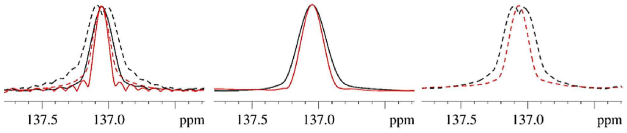

Figure 3. Overlay of 1D sections of the H2–C3 two-bond correlation of ibuprofen. **Left**: *F_1-absorptive* ZQ (red solid) and DQ (black solid) recorded with 30 Hz/point resolution superimposed with *F_1-magnitude* ZQ (red dotted) and DQ (black dotted) recorded with 15 Hz/point resolution. All data were processed without apodization functions. **Middle**: *F_1-absorptive* ZQ and DQ signals obtained after multiplying data with a $\cos^2$ function. **Right**: *F1-magnitude* ZQ and DQ signals obtained after multiplying data with a 30° shifted sine function. All sections were obtained by summing up columns across the peaks and scaled to the same intensity for comparison of multiplet widths. For better visualization expanded signals can be found in the Supplementary Information.

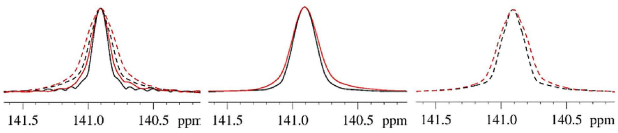

Figure 4. Overlay of 1D sections of the H10–C8 three-bond correlation of ibuprofen. **Left**: *F_1-absorptive* ZQ (red solid) and DQ (black solid) recorded with 30 Hz/point resolution superimposed on *F_1-magnitude* ZQ (red dotted) and DQ (black dotted) recorded with 15 Hz/point resolution. All data were processed without window functions. **Middle**: *F1-absorptive* ZQ and DQ signals obtained after multiplying data with a $\cos^2$ function. **Right**: *F_1-magnitude* ZQ and DQ signals obtained after multiplying data with a 30° shifted sine function.

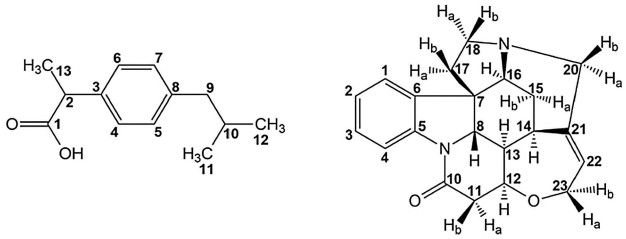

Scheme 1. Structures of ibuprofen (left) and strychnine (right).

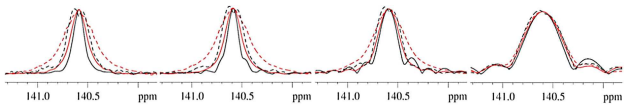

Figure 5. Overlay of 1D sections of the H15a–C21 three-bond correlation of strychnine obtained with digital resolution of 14, 28, 56 and 112 Hz/point (from left to right) in F_1-*absorptive* and 7, 14, 28 and 56 Hz/point in F_1-*magnitude* experiments. The colors and styles of lines are the same as in Figures 3 and 4 and no apodization functions were employed.

two-bond correlation and the opposite is indicative of a three-bond correlation.

The impact of digital resolution from high to coarse resolution is illustrated in Figure 5 for the H15a–C21 correlation in strychnine (right in Scheme 1) in which only little difference is observed in the limit of coarse resolution but there is a clear advantage to the experiment of Figure 2 for high resolution.

In all the above examples, the Difference in Multiplet Width (DMW) of ZQ and 2Q correlations is larger in the F_1-*magnitude* than in the F_1-*absorptive* spectrum. This effect is expected to be exacerbated for strong coupling because the latter experiment includes the final π^H pulse causing mixing of spin states. For the H23a–C21 correlation in strychnine there is strong coupling between the H23a and H23b protons and it is seen in Figure 6

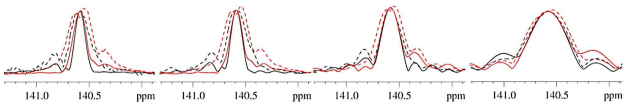

Figure 6. Overlay of 1D sections of the H23a–C21 three-bond correlation of strychnine obtained with digital resolution of 14, 28, 56 and 112 Hz/point (from left to right) in the F_1-*absorptive* and 7, 14, 28 and 56 Hz/point in the F_1-*magnitude* experiments. No apodization functions were employed.

that assignment as a three-bond correlation in the F_1-*absorptive* spectrum can be made safely only for high resolution.

The picture outlined in Figure 1 strictly holds only for two-spin systems, because the final dashed π^H pulse produces complementary E.COSY multiplet patterns,[3] i.e., with all passive spin states inverted. Thus the F_1-*absorptive* SEA XLOC experiment combines normal and complementary E.COSY patterns, and they do not overlap perfectly, which is required for pure absorption profiles. However, as seen in the examples above the technique can deliver clear resolution enhancement, because resolution enhancement occurs even in the case of only partial overlap of normal and complementary E.COSY patterns. It takes relatively large coupling constants of a passive spin to *both* the two active spins for the resolution enhancement to vanish. Such an example is shown in Figure 7 for the H11a–C10 correlation in strychnine in which the two passive coupling constants to H11b are J(H11a–H11b) = −17.2 Hz and J(H11b–C10) = −7.9 Hz. It is seen in Figure 7d that there is not much difference between these corresponding multiplet widths in the spectra recorded with the two methods.

In conclusion, we have presented a way to obtain absorptive profiles and thus resolution enhancement in the

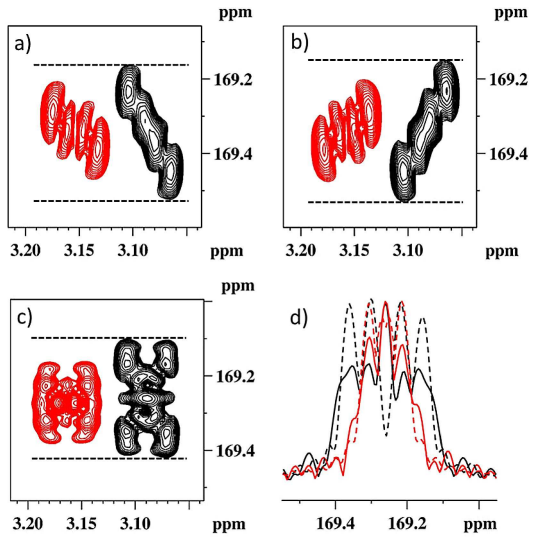

Figure 7. The H11a–C10 two-bond correlation in strychnine. a) and b) obtained using the pulse sequence in Figure 2 without and with the final π^H pulse, respectively, employing a digital resolution of 14 Hz/point and presented in F_1-*magnitude* mode. c) Data in a) and b) combined and spectrum presented in F_1-*absorptive* mode. In the contour plots 2Q peaks (black) are displaced horizontally with respect to ZQ peaks (red) for better visualization. d) 1D sections extracted in analogy to Figures 3–6, i.e. dashed lines from a 7 Hz/point F_1-*magnitude* experiment and full lines from the data in c). The ZQ and 2Q parts are in red and black, respectively, and no apodization functions were employed.

indirect dimension of a 2D SEA XLOC spectrum. The experiment has value for high-resolution applications and when the aim is limited to distinguishing between two- and three-bond correlations. If only a coarse resolution is employed or if coupling constants are to be measured via the original XLOC experiment[4] the first version of SEA XLOC is the one of choice.[1]

Experimental Section

All experiments were performed on a 700 MHz Bruker Avance Neo spectrometer equipped with a TCI z-gradient prodigy probe. ^{1}H and ^{13}C 90° pulses were 7.56 (1 M ibuprofen in $CDCl_3$)/7.99 (0.4 M strychnine in $CDCl_3$) and 12.0 μs, respectively and the sample temperature was 298 K.

SEA XLOC spectra were acquired using the parameters: $\Delta = 83$ ms, $^1J_{min} = 125$ Hz and $^1J_{max} = 165$ Hz, spectral widths of 8.4 ppm (^{1}H) and 180.0 ppm (ibuprofen)/160 ppm (strychnine) (^{13}C), relaxation delay 1.6 s. Ibuprofen: F_1-*magnitude* spectrum was recorded with 2048 increments in t_1 giving a digital resolution of 15 Hz/point, F_1-*absorptive spectrum* was recorded with 1024 increments in t_1 giving a digital resolution of 30 Hz/point, both with 4 scans per increment and 2048 data points in t_2. Strychnine: F_1-*magnitude* spectrum was recorded with 4096 increments in t_1 giving a digital resolution of 7 Hz/point, F_1-*absorptive spectrum* was recorded with 2048 increments in t_1 giving a digital resolution of 14 Hz/point, both with 2 scans per increment and 2048 data points in t_2. The experiment time was about 4 h in all cases.

Acknowledgements

This research was supported by the National Research, Development and Innovation Office of Hungary (grant NKFI/OTKA NN 128368) and co-financed by the European Regional Development Fund (projects GINOP-2.3.3-15-2016-00004, GINOP-2.3.2-15-2016-00044 and GINOP-2.3.2-15-2016-00008) and the ÚNKP-18-3 New National Excellence Program of The Ministry of Human Capacities (TGy).

Conflict of Interest

The authors declare no conflict of interest.

Keywords: NMR spectroscopy · long-range correlation · absorptive profiles · resolution enhancement

[1] T. Gyöngyösi, T. M. Nagy, K. E. Kövér, O. W. Sørensen, *Chem. Commun.* **2018**, *54*, 9781–9784.
[2] A. Bax, D. Marion, *J. Magn. Reson.* **1988**, *78*, 186–191.
[3] a) C. Griesinger, O. W. Sørensen, R. R. Ernst, *J. Am. Chem. Soc.* **1985**, *107*, 5394–6396; b) C. Griesinger, O. W. Sørensen, R. R. Ernst, *J. Chem. Phys.* **1986**, *85*, 6837–6852; c) C. Griesinger, O. W. Sørensen, R. R. Ernst, *J. Magn. Reson.* **1985**, *75*, 474–492.
[4] a) M. D. Sørensen, S. M. Kristensen, J. J. Led, O. W. Sørensen, *J. Magn. Reson. Ser. A* **1993**, *103*, 364–368; b) M. D. Sørensen, J. J. Led, O. W. Sørensen, *J. Biomol. NMR* **1994**, *4*, 135–141; c) H. Thøgersen, O. W. Sørensen, *J. Magn. Reson. Ser. A* **1994**, *110*, 118–120; d) A. Meissner, O. W. Sørensen, *Magn. Reson. Chem.* **2001**, *39*, 49–52; e) T. Schulte-Herbrüggen, A. Meissner, A. Papanikos, M. Meldal, O. W. Sørensen, *J. Magn. Reson.* **2002**, *156*, 282–294.

Manuscript received: April 16, 2019
Revised manuscript received: May 26, 2019